CHAPTER

7 Elastic-Plastic Fracture Criteria

We have learned from Sections 3.9 and 4.1 that (quasistatic) crack growth in perfectly elastic materials can be predicted by the stress intensity factor criterion or equivalently the energy release rate criterion. Under a narrowly defined small-scale yielding (SSY) condition, that is, the plastic deformation is confined in the K-dominance zone of the linear elastic fracture mechanics (LEFM), the stress intensity factor or energy release rate can be used to predict fracture in elastic-plastic materials. The high fracture toughness for metals (Table 3.1 in Section 3.9) indeed results from the energy dissipation in the small plastic zone. When the "strict" SSY condition is not satisfied but the plastic deformation is still confined in the crack tip region, the LEFM approach may still be used by adopting Irwin's adjusted stress intensity factor concept.

Prediction of quasistatic crack growth (including crack initiation and extension) has not been as successful as that in LEFM when large-scale yielding (LSY) conditions prevail, that is, the size of the plastic zone at crack initiation and during crack growth is comparable to, or larger than, the crack length or other in-plane dimensions. In the case of LSY, parameters that describe the overall plastic deformation around the crack tip are needed for crack growth prediction. These parameters include the crack opening displacement (COD), crack tip opening angle (CTOA), and others. This chapter introduces various fracture criteria for predicting quasistatic crack growth in materials undergoing plastic deformations.

7.1 IRWIN'S ADJUSTED STRESS INTENSITY FACTOR APPROACH

Irwin's model introduced in Section 6.3 suggets that the adjusted stress intensity factor with the plastic zone size may be used to predict fracture in elastic-plastic materials under moderate yielding conditions. For this reason, Irwin's approach is also introduced in the LEFM part of most fracture mechanics books. To introduce Irwin's adjusted stress intensity factor approach, we first look at, as shown in Figure 7.1 [7-1], the stress distributions σ_{yy} along the crack line in a center-cracked plate (plane stress) as predicted from Irwin's model and the finite element calculations for an elastic-perfectly plastic material.

Fracture Mechanics. DOI: 10.1016/B978-0-12-385001-0.00007-9

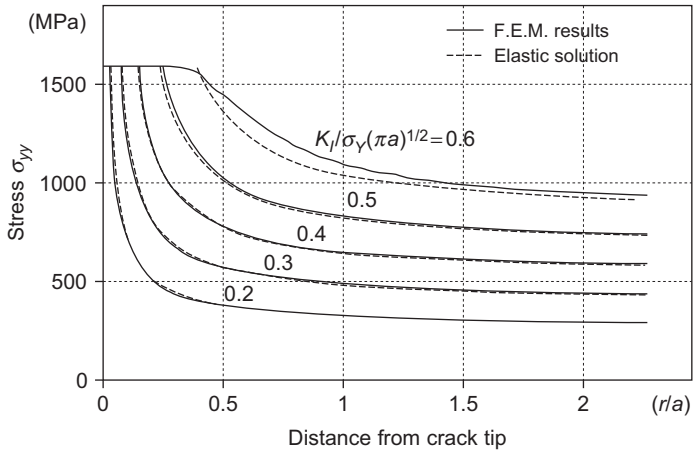

FIGURE 7.1

Stress distribution in front of the crack as predicted from Irwin's model and the finite element method (adapted from Kim [7-1]).

It can be seen that the stress of Irwin's model closely matches the finite element results for load levels up to $K_I/(\sigma_Y\sqrt{\pi a}) = 0.5$, implying that Irwin's model may be used beyond the SSY limitations. Here, K_I is the applied stress intensity factor, σ_Y is the yield stress, and a is half the crack length. Because the stress field around the crack tip in Irwin's model is characterized by the adjusted stress intensity factor, $K_I(a_{eff})$, using the effective crack length a_{eff}, the crack growth condition may be formulated as follows:

$$K_I(a_{eff}) = K_c \tag{7.1}$$

where a_{eff} is the effective crack length given by Eq. (6.38) in Chapter 6 and K_c is a material constant. This K_c should not be confused with the fracture toughness discussed in Chapter 3. This K_c also depends on the thickness of the material.

Irwin's adjusted stress intensity approach has often been labeled in the literature as an SSY approach. The SSY has been frequently referred to and used in general fracture mechanics studies. Hence the SSY concept merits further discussion. The SSY usually means that the crack tip plastic zone is so small that the stress intensity factor in LEFM is applicable. Based on this understanding, the K-dominance zone exists near a crack tip and the plastic zone extends to only a fraction of the K-dominance zone size, as schematically shown in Figure 7.2. The SSY Mode III solution in Section 6.7 is studied based on this assumption.

A broadly defined SSY, or an extension of the previous narrowly defined SSY, may originate from Irwin's model. In this case, the stress intensity factor is still applicable, but modified by using Irwin's effective crack length. Now the plastic zone size may not be negligible compared with the crack length, or other in-plane dimensions.

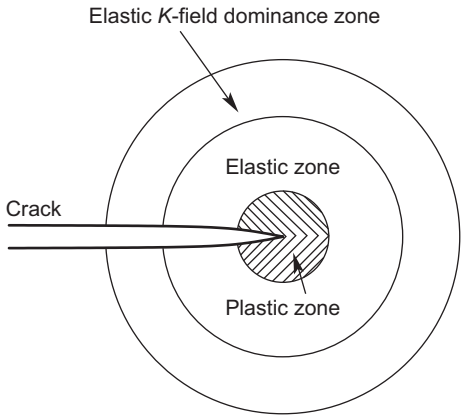

FIGURE 7.2

Schematic of crack tip SSY.

The stress distributions σ_{yy} shown in Figure 7.1 indicate that Irwin's model may be used for materials undergoing moderate plastic yielding. Irwin's adjusted stress intensity factor is generally larger than the stress intensity in LEFM. For a crack in an infinite plate under uniform remote tension, for example, the adjusted stress intensity factor is given by Eq. (6.39):

$$K_I(a_{eff}) = \sigma\sqrt{\pi a}/\sqrt{1-\frac{1}{2}\left(\frac{\sigma}{\sigma_Y^*}\right)^2}$$

7.2 *K* RESISTANCE CURVE APPROACH

The K_R curve approach is also commonly characterized as an LEFM fracture criterion as the stress intensity factor K is employed. The K_R curve behavior, however, is a result of increased energy dissipation in the plastic zone that grows with crack extension. If we measure the stress intensity factor K for an elastic-plastic material (especially a thin sheet) with a crack, we will observe that the stress intensity factor increases with crack growth as shown in Figure 7.3, where a_0 is the initial crack size, $a - a_0$ is the crack extension, and K_i is the critical stress intensity factor at crack initiation. The crack growth in the material is thus stable before the final failure occurs.

This is the so-called K resistance curve behavior, or simply K_R curve behavior. Materials, particularly thin-sheet materials, with high fracture toughness and low-yield strength, exhibit K_R curve behavior because a relatively larger plastic zone develops around the crack tip. Now the fracture resistance force is characterized by

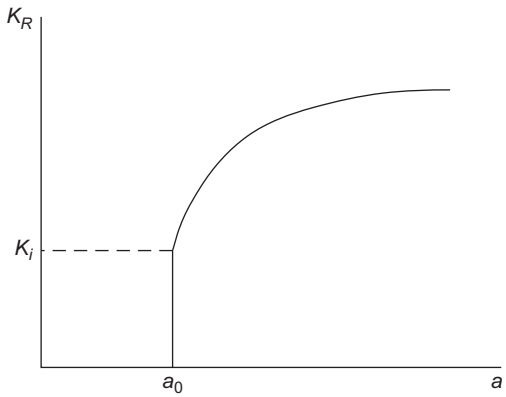

FIGURE 7.3

K resistance curve.

a curve of K_R versus crack extension instead of a single parameter K_c. It is obvious that the resistant curve can be expressed alternately in energy release rate G.

For a material exhibiting K_R curve behavior, failure is determined not only by the comparison between the applied K and K_R, but also by the comparison between the slopes of the applied K and K_R curve. Unstable crack growth takes place when the following two conditions are met:

$$\begin{aligned} K_I(a) &= K_R(\Delta a), \\ \frac{dK_I(a)}{da} &= \frac{dK_R(\Delta a)}{d(\Delta a)} \end{aligned} \tag{7.2}$$

The first equation in Eq. (7.2) is equivalent to Eq. (7.1) but is taken at the current crack length. The second equation in Eq. (7.2) implies that the applied K will continue to exceed K_R for a small crack extension from the current crack length (initial length plus crack extension).

Figure 7.4 shows the K_R curve and a set of fracture driving force curves at different load levels for a given cracked specimen with an initial flaw size a_0. No crack growth occurs at load level P_1 because the applied K is always lower than the K_R for the crack length considered. The crack initiation takes place when the load reaches P_2, as $K(P_2) = K_R(a_0)$ at $a = a_0$. The crack growth, however, is stable as the slope of the driving force curve is smaller than that of the K_R curve at $a = a_0$. The crack extension stops, as $K(P_2)$ is lower than K_R for longer cracks. At the load level P_3, unstable crack growth occurs because both conditions in Eq. (7.2) are met.

It is important to note that condition Eq. (7.2) holds only for the SSY cases, that is, a K-dominance zone exists and is characterized by the stress intensity factor based on the physical crack length. When the SSY condition is not satisfied, Irwin's adjusted

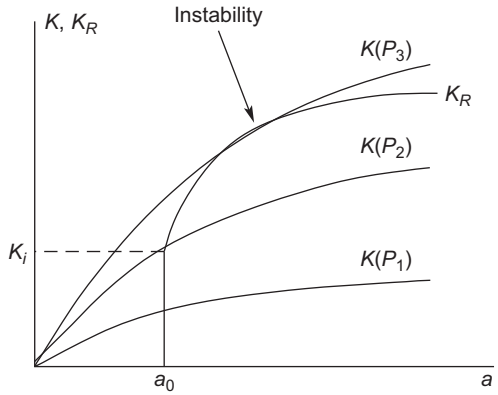

FIGURE 7.4

Fracture instability determined from the driving and resistance curves.

crack length a_{eff} should be used and the criterion Eq. (7.2) now becomes

$$\begin{aligned} K_I(a_{eff}) &= K_R(\Delta a_{eff}), \\ \frac{dK_I(a_{eff})}{da_{eff}} &= \frac{dK_R(\Delta a_{eff})}{d(\Delta a_{eff})} \end{aligned} \tag{7.3}$$

Bray et al. [7-2] studied the K_R curves for an aluminum alloy (C188-T3) using center-cracked tension (or middle-crack tension, M(T)) specimens as shown in Figure 7.5. The K_R curve may be determined from

$$K_R(\Delta a_{eff}) = \frac{P}{BW}\sqrt{\pi a_{eff}}F\left(\frac{2a_{eff}}{W}\right), \quad F(\alpha) = 1 + 0.128\alpha - 0.288\alpha^2 + 1.525\alpha^3$$

where P is the applied load corresponding to the crack extension, W is the width, B is the thickness, $2a$ is the physical crack length, and $2a_{eff}$ is the effective crack length.

Figure 7.6 shows the K_R versus effective crack growth curves for aluminum specimens with a width of 6.3, 16, and 60 inches, respectively. It can be seen that the K_R curves are basically independent of the specimen size, which indicates that the K_R curve in terms of the effective crack extension is a material property. Of course, the K_R curve is thickness dependent. Figure 7.7 shows the K_R curves based on the physical crack growth for the aluminum specimens. The K_R curve now depends on the specimen size, that is, different specimen sizes result in different K_R curves. Hence, the K_R curve is not a material property if it is based on the physical crack length. The reason is that the plastic zone is not small in this case, which invalidates the use of physical crack length.

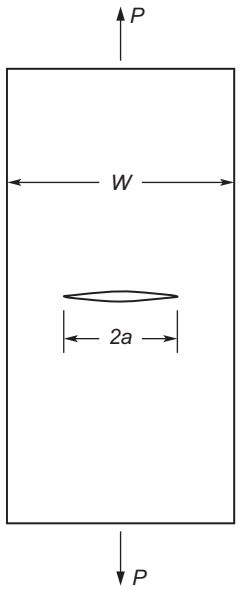

FIGURE 7.5

A center-cracked specimen in tension.

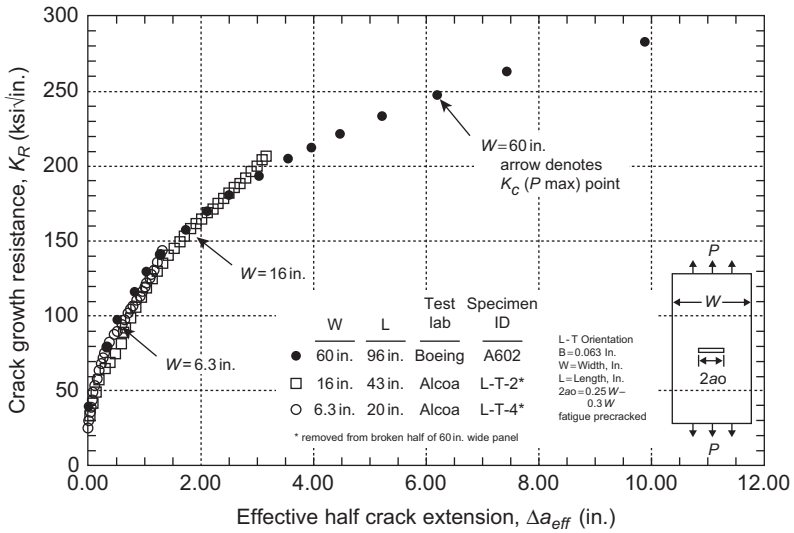

FIGURE 7.6

K_R curves for C188-T3 aluminum with different specimen sizes using the effective crack length (adapted from Bray et al. [7-2]).

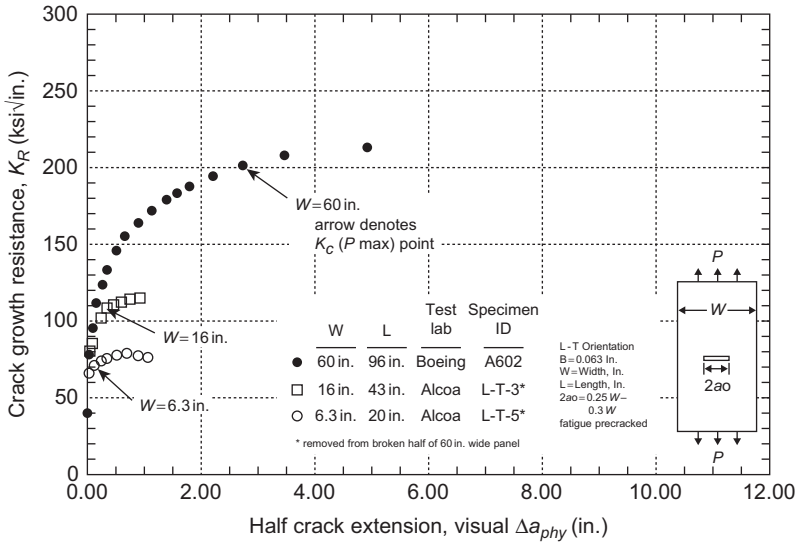

FIGURE 7.7

K_R curves for a center-cracked specimen with different specimen sizes using the physical crack length (adapted from Bray et al. [7-2]).

7.3 *J*-INTEGRAL AS A FRACTURE PARAMETER

The HRR field in Eqs. (6.140) through (6.142) in Section 6.9 of Chapter 6 indicates that the J-integral describes the intensity of the near-tip singular stress and deformation fields for a power-law hardening material similar to the way that the stress intensity factor describes the stress and strain intensity in linear elastic materials. A natural extension of the stress intensity factor methodology to the elastic-plastic fracture mechanics is to use J as a fracture parameter. Begley and Landes [7-3] proposed the following elastic-plastic crack initiation condition based on this concept:

$$J = J_{Ic} \tag{7.4}$$

where J_{Ic} is the critical value of J at crack initiation for plane strain. J_{Ic} should be a material property and determined by experiment. Under SSY conditions, we have the relation between J and stress intensity factor (plane strain Mode I):

$$J = \frac{1-\nu^2}{E} K_I^2$$

Thus, the J criterion is equivalent to the stress intensity factor criterion in SSY.

Under LSY conditions, however, applications of J to predicting elastic-plastic fracture have been limited due to several factors. First, the HRR field is based on

the deformation theory of plasticity. Deformation plasticity generally requires proportional loading and thus applies to cracked bodies subjected to monotonically increasing loads. Once crack growth occurs, unloading takes place in the wake region along the crack faces, which invalidates the deformation plasticity. As a result, J may be used only for predicting crack initiation but not crack growth in general. Some studies (e.g., Hutchinson and Paris [7-4]), however, suggested that J may be used to predict crack extension if the extension amount is small so that an HRR-dominance zone still exists.

Second, for J to be the sole parameter to describe the stress and deformation intensity near a stationary crack tip, the HRR singular solution must dominate the stress field there. In ductile fracture of metals, large deformations are significant around the crack tip as evidenced by crack tip blunting. The HRR-dominance zone must not fall into the region where large deformations are significant because the small deformation assumption is used in establishing the HRR field. The dominance of the HRR field depends on strain hardening properties as well as configurations of cracked specimens.

The dominance of the HRR field deteriorates significantly for weakly hardening materials. When $n >> 1$, the stress singularity exponent $-1/(n+1)$ becomes very small, which allows other terms in the asymptotic stress solution to be comparable to the HRR stress field. Finite element analyses of the crack tip deformation (e.g., McMeeking and Parks [7-5] and Shih and German [7-6]) for plane strain showed that the HRR field exists for the single-edge notched bend and double-edge notched tension specimens with hardening exponent $n = 10$ when the following condition is approximately met:

$$\frac{b\sigma_Y}{J} \geq 30 \tag{7.5}$$

where b is the ligament size and σ_Y is the yield stress. For the single-edge notched tension or center-cracked tension specimens with $n = 10$, however, the HRR field may exist only when

$$\frac{b\sigma_Y}{J} \geq 200 \tag{7.6}$$

Inequalities Eqs. (7.5) and (7.6) mean that the J-integral may be used to predict crack initiation for LSY under some restrictive conditions.

7.4 CRACK TIP OPENING DISPLACEMENT CRITERION

In LEFM, the near-tip stress and strain fields are always characterized by the inverse square-root singularity and the stress intensity factor is a fracture parameter for both crack initiation and propagation. In elastic-plastic fracture mechanics, however, it is much more difficult to find a similar parameter directly characterizing the intensity of the near-tip singular deformation field for both stationary and growing cracks under LSY conditions. For example, the K_R curve concept based on the effective crack

length may not be applied when the plastic zone touches the specimen boundary. Also, the J-integral theoretically holds only for stationary cracks.

On the other hand, parameters describing the near-tip crack profile have been suggested for predicting fracture because the crack profile near the tip reflects the overall severity of the plastic deformation. The crack tip opening displacement (CTOD) and the crack tip opening angle (CTOA) approaches have gained much attention in recent years and proved promising as fracture parameters for both crack initiation and extension prediction. This section describes the CTOD concept and the CTOA approach is discussed in the next section.

According to the CTOD method (Wells [7-7]), the Mode I crack initiation occurs once the the following condition is met:

$$\delta = \delta_c \tag{7.7}$$

where δ is the CTOD, and δ_c is the critical value of the CTOD and is determined by experiments. Once the CTOD is calculated for a cracked structure, Eq. (7.7) may be used to predict the failure load for a given crack size.

Calculation of CTOD according to Irwin's model was discussed in Section 6.3. The result is

$$\delta = \frac{4}{\pi E^*} \frac{K_I^2}{\sigma_Y^*} \tag{7.8}$$

where $E^* = E$ and $\sigma_Y^* = \sigma_Y$ for plane stress, and $E^* = E/(1-\nu^2)$ and $\sigma_Y^* = \sigma_Y/(1-2\nu)$ for plane strain. A relation between δ and K_I was also established using the Dugdale model in SSY in Section 6.4:

$$\delta = \frac{K_I^2}{E^* \sigma_Y^*} \tag{7.9}$$

For SSY, we may have a general relationship between the CTOD and the stress intensity factor as follows:

$$\delta = \beta \frac{K_I^2}{E^* \sigma_Y^*} \tag{7.10}$$

where β is a parameter of order unity equal to 1 according to the Dugdale model and $4/\pi$ according to Irwin's model. The relation between the CTOD and the stress intensity factor indicates that the CTOD criterion is equivalent to the stress intensity criterion in SSY.

Under LSY conditions, the CTOD may be obtained in closed form using the Dugdale model. Otherwise, the finite element method is used to obtain the crack tip opening displacement value. For a crack in an infinite plate subjected to remote

tension σ, the CTOD according to the Dugdale model is given by

$$\delta = -\frac{8a\sigma_Y^*}{\pi E^*} \ln\left(\cos\frac{\pi\sigma}{2\sigma_Y^*}\right) \tag{7.11}$$

Using Eqs. (7.7) and (7.11), the crack extension condition becomes

$$-\frac{8a\sigma_Y^*}{\pi E^*} \ln\left(\cos\frac{\pi\sigma}{2\sigma_Y^*}\right) = \delta_c$$

For a given crack length $2a$, the failure applied stress is obtained from the preceding equation:

$$\sigma_f = \frac{2}{\pi}\sigma_Y^* \cos^{-1}\left[\exp\left(-\frac{\pi E^*\delta_c}{8a\sigma_Y^*}\right)\right]$$

For a given applied load, the allowable crack length becomes

$$2a = -\frac{\pi E^*\delta_c}{4\sigma_Y^*} / \ln\left(\cos\frac{\pi\sigma}{2\sigma_Y^*}\right)$$

In the Dugdale or Irwin's model, the CTOD can be determined unambiguously as the crack opening at the physical crack tip. For general ductile fracture problems, a proper definition of CTOD is required. For ductile materials, significant crack tip blunting occurs at crack initiation. Figure 7.8 shows a blunted crack tip region versus the initially sharp crack tip. The CTOD by definition is the crack opening displacement at the orginal sharp crack tip, as shown in Figure 7.8. This definition, however, is not convenient for numerical computations.

Tracy [7-8] proposed a 45° interception definition of CTOD for stationary cracks, as shown in Figure 7.9. The CTOD is now the crack opening at the point at which the crack faces intercept the straight lines of 45° emanating from the blunted crack tip. Using the 45° interception definition and the HRR field, Shih [7-9] derived a relation between the J-integral and CTOD as follows:

$$\delta = d_n \frac{J}{\sigma_Y}$$

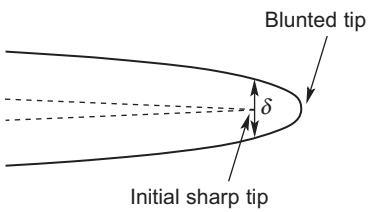

FIGURE 7.8

CTOD definition based on the original crack tip position.

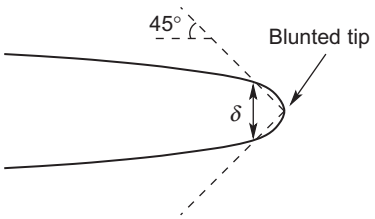

FIGURE 7.9

CTOD definition based on the 45° intercept assumption.

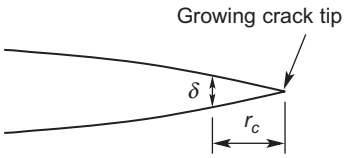

FIGURE 7.10

CTOD definition based on a characteristic distance r_c.

where d_n is a constant depending on the yield strain and the power-hardening exponent n. It should be noted that this relation is valid only when the HRR solution dominates the crack tip stress and deformation fields.

For growing cracks, the crack tip blunting is not significant. Theoretical analyses of near-tip fields around a growing crack in a perfectly plastic material (Rice [7-10]) show that the opening at the growing crack tip vanishes. In this case, the following modified CTOD criterion may be used:

$$\delta = \delta_c, \quad \text{at } r = r_c$$

where r_c is a characteristic distance from the crack tip, as shown in Figure 7.10. In engineering applications, r_c may be calibrated by matching the predicted crack growth response using the preceding criterion with the experimentally measured one. It will be seen in the following section that the CTOD criterion based on the length parameter r_c is actually equivalent to the CTOA criterion.

7.5 CRACK TIP OPENING ANGLE CRITERION

Similar to CTOD, the CTOA is also a parameter describing the overall severity of plastic deformation in the near-tip region. Theoretically, CTOA is defined as the angle between the two crack faces at the crack tip:

$$\text{CTOA} = \psi = 2\tan^{-1}\left(\frac{\delta_0}{2r_0}\right) \tag{7.12}$$

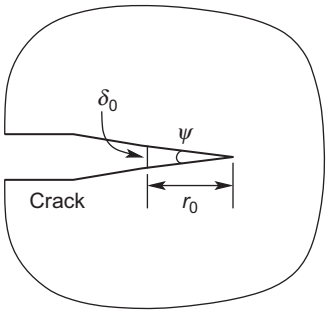

FIGURE 7.11

CTOA definition.

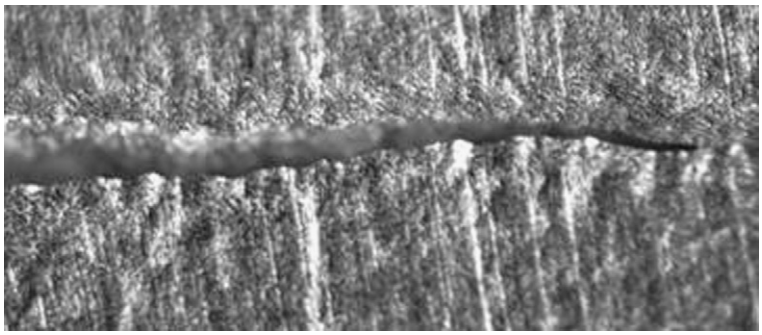

FIGURE 7.12

Crack profile in an aluminum alloy.

where δ_0 is the crack opening displacement at distance r_0 behind the crack tip, as shown in Figure 7.11. If the crack faces follow perfect straight lines in the near-tip region, the CTOA will not depend on the selection of r_0. In real materials, however, the crack faces follow meandering paths. In this case, the CTOA is defined as the average value of the crack opening angle over a small distance behind the crack tip. Figures 7.12 and 7.13 show the crack profiles in the near-tip region for an aluminum alloy and a duplex steel, respectively. It can be seen from the figure that CTOA can be well-defined for the crack growth in the steel, but an averaged CTOA must be used for the aluminum alloy.

According to the CTOA criterion, crack extension occurs when

$$\text{CTOA} = \psi_c \tag{7.13}$$

where ψ_c is the critical CTOA and is determined by experiment.

FIGURE 7.13

Profile of a crack after growth of 5 mm in a duplex steel.

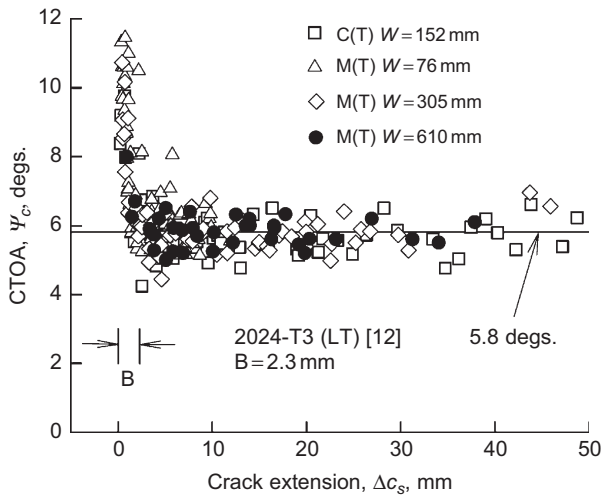

FIGURE 7.14

Measured CTOA data for crack growth in thin sheet, aluminum 2024-T3 specimens (adapted from Newman et al. [7-12]).

The CTOA criteron has gained much attention in recent years in the study of fracture processes in ductile materials (Newman and Zerbst [7-11]). To simulate ductile fracture using the CTOA criterion, the critical CTOA, ψ_c, in Eq. (7.13) needs to be experimentally determined. Figure 7.14 shows the measured critical CTOA values versus crack extension on the surface, Δc_s, for a thin-sheet aluminum alloy (Newman et al. [7-12]). Results for both compact tension (C(T)) and middle-crack

tension (M(T)) specimens are included. The specimens have different widths (W) but the same thickness of 2.3 mm.

It can be observed from the figure that (1) the critical CTOA at crack initiation is much higher than that during crack extension; (2) the critical CTOA decreases rapidly with increasing crack extension at the initial growth stage and approximately reaches a constant value of about 5.8 degrees after a small amount of crack growth; and (3) the critical CTOAs for different specimens basically fall in a narrow band, which indicates the existence of a CTOA versus crack extension curve (CTOA resistance curve) that is independent of specimen size and geometry. Hence, the CTOA curve may be regarded as a material property.

Elastic-plastic fracture criteria typically are thickness-dependent, that is, the critical value of the fracture parameter varies with specimen thickness. This has been known for the criterion based on Irwin's model of adjusted stress intensity factor. Mahmound and Lease [7-13] measured the critical CTOA values on the surface of C(T), 2024-T351 aluminum alloy specimens with thicknesses from 2.3 to 25.4 mm. All the specimens have the same width of 203 mm. Their results confirmed the basic characteristic of CTOA curve behavior for all specimens of different thicknesses, that is, for a given specimen, the CTOA has a high value at crack initiation, decreases rapidly and reaches a constant value after a small amount of crack extension. The CTOA curve, however, depends on the specimen thickness.

Figure 7.15 shows the variation of critical CTOA values in the constant region with specimen thickness (Mahmound and Lease [7-13]). The results for thin-sheet

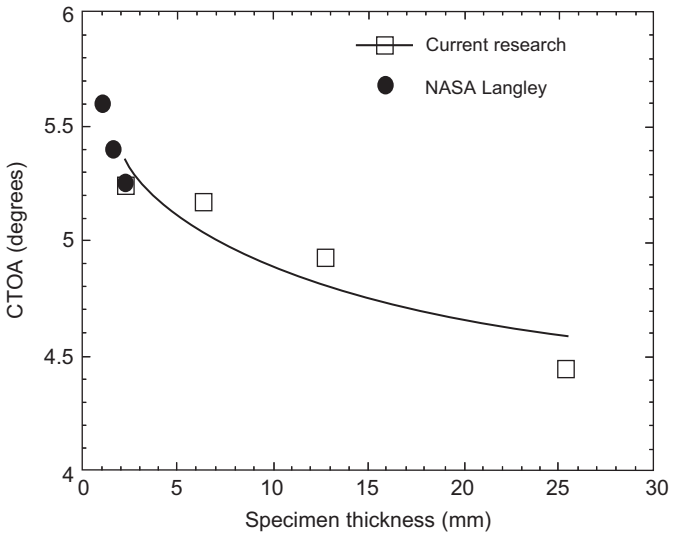

FIGURE 7.15

Thickness dependence of critical CTOA (in the constant region) for 2024-T351 aluminum alloy (adapted from Mahmoud and Lease [7-13]).

specimens in earlier NASA studies are also included. The critical CTOA values are about 5.24, 5.17, 4.92, and 4.48 degrees for the specimens 2.3, 6.35, 12.7, and 25.4 mm thick, respectively. Hence, the critical CTOA decreases with an increase in specimen thickness. Does the CTOA approach a constant value for specimens of large thickness? It appears that the answer is yes, but further experimental work needs to be done in the future.

Simulation of ductile fracture from crack initiation to extension using the CTOA criterion generally requires employment of the entire CTOA curve. Newman et al. [7-12], however, used a constant CTOA value (the CTOA in the constant region) from crack initiation to extension to simulate the load versus crack extension responses. They found that while neither the plane stress nor plane strain model produced results that matched the measured response, the three-dimensional modeling results matched the measured response by using a constant CTOA value. They attributed the phenomenon to the three-dimensional constraint effects and crack tunneling as the measured CTOA data is for the specimen surface and it is larger than that in the specimen interior.

References

[7-1] H-O. Kim, Elastic-plastic fracture analysis for small scale yielding, PhD thesis, School of Aeronautics and Astronautics, Purdue University, West Lafayette, Indiana, 1996.

[7-2] G.H. Bray, R.J. Bucci, J.R. Weh, Y. Macheret, Prediction of wide-cracked-panel toughness from small coupon tests, in: Advanced Aerospace Materials/Process Conference, Anaheim, CA, 1994.

[7-3] J.A. Begley, J.D. Landes, The *J*-integral as a fracture criterion, Fracture Toughness, Part II, ASTM STP 514, in: American Society for Testing and Materials, Philadelphia, 1972, pp. 1–20.

[7-4] J.W. Hutchinson, P.C. Paris, Stability analyses of *J* controlled crack growth, Elastic-Plastic Fracture, ASTM STP 668, in: American Society for Testing and Materials, Philadelphia, 1979, pp. 37–64.

[7-5] R.M. McMeeking, D.M. Parks, On criterion for *J*-dominance of crack tip fields in large scale yielding, Elastic-Plastic Fracture, ASTM STP 668, in: American Society for Testing and Materials, Philadelphia, 1979, pp. 175–194.

[7-6] C.F. Shih, M.D. German, Requirements for a one parameter characterization of crack tip fields by the HRR singularity, In. J. Fract. 17 (1981) 27–43.

[7-7] A.A. Wells, Application of fracture mechanics at and beyond general yielding, Br. Weld. J. 11 (1961) 563–570.

[7-8] D.M. Tracy, Finite element solutions for crack tip behavior in small scale yielding, ASME J. Eng. Mater. Technol. 98 (1976) 146–151.

[7-9] C.F. Shih, Relationship between the *J*-integral and crack opening displacement for stationary and growing cracks, J. Mech. Phys. Sol. 29 (1981) 305–326.

[7-10] J.R. Rice, Elastic-plastic crack growth, in: H.G. Hopkins, M.J. Sewell (Eds.), Mechanics of Solids, Pergamon, Oxford, UK, 1982, pp. 539–562.

[7-11] J.C. Newman Jr., U. Zerbst, Engineering fracture mechanics, Eng. Fract. Mech. 70 (2003) 367–369.

[7-12] J.C. Newman Jr., M.A. James, U. Zerbst, A review of the CTOA/CTOD fracture criterion, Eng. Fract. Mech. 70 (2003) 371–385.

[7-13] S. Mahmoud, K. Lease, The effect of specimen thickness on the experimental characterization of critical crack tip opening angle in 2024-T351 aluminum alloy, Eng. Fract. Mech. 70 (2003) 443–456.

PROBLEMS

7.1 A thin plate with a center crack is loaded with uniform tensile stresses as shown in Figure 7.16. The elastic-perfectly plastic ductile material has Young's modulus of 70 GPa and yield stress of 400 MPa. Fracture tests are conducted and failure is found to occur when the net section stress reaches the yield stress. Plot the applied stress at failure as a function of a/W. If the net-section failure is interpreted as fracture failure, find fracture toughness K_c using Irwin's plastic zone adjustment method and plot it as a function of a/W. This plot will indicate that K_c is specimen size dependent and is not suitable for characterizing this type of "ductile fracture."

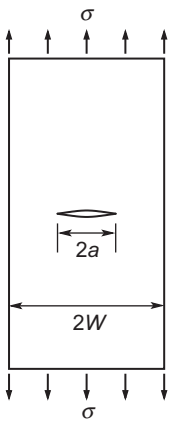

FIGURE 7.16

A center-cracked plate under tension.

7.2 Find the critical applied stress for unstable crack extension in an edge-cracked specimen (see Figure 7.17) made of a C188-T3 aluminum using the K_R curve shown in Figure 7.6. Assume that the crack length is $a = 50$ cm, the specimen

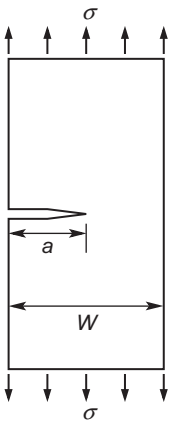

FIGURE 7.17

An edge-cracked plate under tension.

width is $W = 200\,\text{cm}$, and the specimen length is much larger than the width. Use the following stress intensity factor formula for the edge-crack problem:

$$K_I = \sigma\sqrt{\pi a}(1.12 - 0.231\alpha + 10.55\alpha^2 - 21.72\alpha^3 + 30.39\alpha^4),\ \alpha = a/W \leq 0.6$$